Available online at www.sciencedirect.com
ScienceDirect
Mendeleev Commun., 2013, **23**, 331–333
Mendeleev Communications

Chemical composition of Fe–Mo alloys obtained by electrodeposition

Vitaly V. Kuznetsov,*[a] Konstantin E. Golyanin,[a] Tatiana V. Pshenichkina,[a] Boris F. Lyakhov[b] and Svetlana E. Lyashenko[a]

[a] *Department of Electrochemistry Engineering, D. I. Mendeleev University of Chemical Technology of Russia, 125047 Moscow, Russian Federation. Fax: +7 499 978 8660; e-mail: vitkuzn1@mail.ru*
[b] *A. N. Frumkin Institute of Physical Chemistry and Electrochemistry, Russian Academy of Sciences, 119071 Moscow, Russian Federation*

DOI: 10.1016/j.mencom.2013.11.009

Iron–molybdenum alloys prepared by electrodeposition from ammonia-citrate solutions contain iron and molybdenum in metallic states and a large amount of sorbed hydrogen.

The electrodeposition of alloys is important for modern chemistry.[1] Iron–molybdenum alloys were used as catalysts in practically important processes such as hydrocarbon conversion,[2] methanol oxidation to formaldehyde[3] and NO reduction.[4] Fe–Mo cathodes can also be used for electrochemical hydrogen evolution.[5,6] Electrochemical methods can be applied to the production of Fe–Mo alloys.[7,8] A hypothesis had been made[9] suggesting that a surface film consisting of molybdenum oxides is formed at the cathode during the initial electrolysis stages, which is an essential prerequisite for alloy electrocrystallization. Due to the formation of molybdenum oxides, the deposits obtained at early electrolysis stages contain high quantities of Mo. The aim of this work was to examine the formation of Fe–Mo deposits from ammonia-citrate solutions, which make it possible to obtain coatings with high molybdenum content.

The Fe–Mo alloy was electrodeposited on the surface of copper and steel samples in the potentiostatic and galvanostatic modes from the solutions containing $Fe_2(SO_4)_3 \cdot 9H_2O$ (0.10 mol dm^{-3}), $Na_2MoO_4 \cdot 2H_2O$ (0.04 mol dm^{-3}), citric acid (0.28 mol dm^{-3}), and NH_4Cl (0.20 mol dm^{-3}) at pH 3.0. The solutions prepared from Fe^{II} salts were unstable because of oxidation of Fe^{II} citrate complexes by Mo^{VI} compounds. Due to this phenomenon all solutions applied for Fe–Mo electrodeposition were prepared from Fe^{III} compounds. Baths containing Fe^{III} complexes were described earlier.[10,11] Potentiostatic studies were carried out in a three-electrode electrochemical cell, the working electrode potential was measured *vs*. an Ag/AgCl reference electrode. All potentials are given *vs*. a standard hydrogen electrode (SHE). An electrode from platinized titanium was used as an anode. The cathode and anode compartments were separated using a Nafion® membrane. During the electrodeposition process, we recorded the dependence of the current flowing through the electrode on electrolysis time (at E = const). The chemical compositions of the cathode deposits were determined by their dissolution in concentrated nitric acid and the analysis of the solution obtained by inductively coupled plasma atomic emission spectroscopy (ICP AES); the average thickness of deposits was 10 μm. The chemical compositions of the surface layers and the valence states of the elements in them were determined by X-ray photoelectron spectroscopy (XPS) (AlKα radiation), the identification of spectra was performed according to a published procedure.[12] The phase composition was determined using X-ray diffraction (XRD) analysis (CuKα radiation); a diffracted-beam graphite monochromator was used to minimize the contribution of fluorescent radiation.

The electrochemical deposition of the Fe–Mo alloy is possible only at potentials more negative than –0.92 V. At E < –0.95 V, the cathode current efficiencies of iron and molybdenum electrodeposition reactions were weakly dependent on the cathode potential (current density) (Table 1). A significant part of cathode current had gone on electrochemical evolution of hydrogen. Hydrogen evolution while electrolysis processing can result in the considerable hydrogenation of deposits obtained.

Table 1 Current efficiencies of iron and molybdenum deposition and hydrogen evolution at different electrode potentials.

–E/V	Current efficiency (%)		
	Fe	Mo	Fe/Mo
0.92	1.8	2.7	1.3
0.95	6.8	10.5	1.3
0.97	7.7	11.2	1.4
1.01	8.2	12.4	1.3
1.08	7.9	12.9	1.2

The coatings deposited at E < –0.95 V contained iron and molybdenum only in metal states (Figure 1). Iron and molybdenum oxides were detected only in the surface layers of deposits ($\delta \leqslant 20$ nm). They formed due to contact of electrodeposited

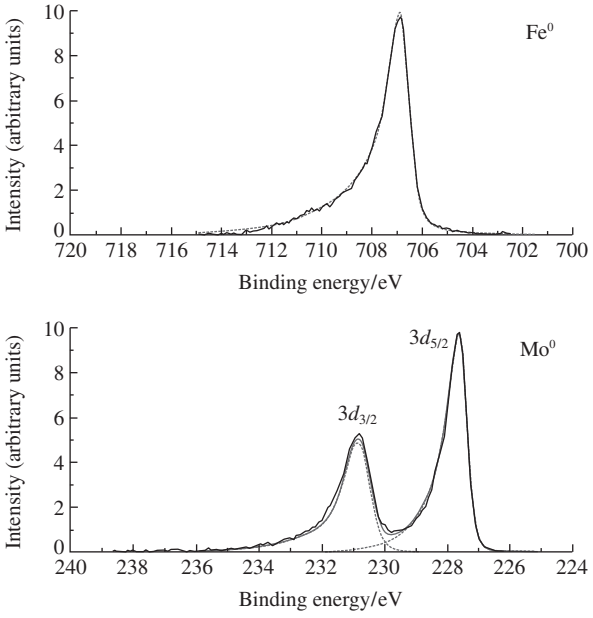

Figure 1 Fe 2*p* and Mo 3*d* XPS spectra. Analytical depth, 60 nm; E_{dep}, –1.00 V.

Table 2 Chemical composition of Fe–Mo deposits (XPS data) (at%).

Analytical depth/nm	C 1*s*	O 1*s*	Mo 3*d*	Fe 2*p*	Fe/Mo
0	29.3	42.4	0.5	3.4	7.6
10	2.3	31.7	9.0	28.3	3.2
20	3.4	23.4	17.4	37.1	2.1
60	<0.2	10.1	28.7	48.2	1.7
80	<0.2	9.6	29.4	49.4	1.7

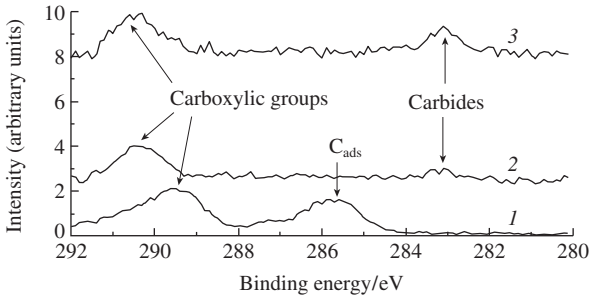

Figure 2 C 1*s* XPS spectra. Analytical depth: (*1*) 0, (*2*) 10 and (*3*) 20 nm. E_{dep}, –1.00 V.

alloys with air. Note that these oxides play an important role in catalysis[3] and electrocatalysis.[13]

Some discrepancy in the data of Tables 1 and 2 (Fe/Mo ratio) can be explained taking into account that values in Table 2 correspond to surface layers, whereas those in Table 1 relate to the entire deposit (~10000 nm in thickness). The discrepancy can also be connected with disadvantages in the determinations of atomic portions of elements from overview XPS spectra.[12]

An amount of carbon detected on the deposit surface (Table 2, Figure 2) is attributed to organic substances adsorbed from air (285.7 eV); another part of carbon at the surface most likely corresponds to carboxyl groups (290 eV). After ion-beam etching, the peak corresponding to adsorbed hydrocarbons disappeared completely, and the second peak shifted to 290.5 eV. This proves that this carbon corresponds to carboxyl groups. Moreover, a high-resolution XPS spectrum revealed a weakly pronounced peak, which is characteristic of carbides (283 eV).

Apparently, the destruction of citrate ions accompanied by the inclusion of carbon-containing compounds into the cathode deposit occurred during Fe–Mo alloy electrodeposition. However, note that this process is negligible because of an almost zero carbon content of the cathode deposit (Table 2).

All the Fe–Mo alloys obtained were X-ray amorphous (Figure 3), their diffractograms showed only highly vague and diffuse reflection, apparently, corresponding to α-Fe. Reflections corresponding to molybdenum were not observed. This fact evidences the assumption that the electrodeposited materials are the solid solutions of molybdenum supersaturated in α-Fe phase. The amorphization of cathode deposits was supposed to be caused by their hydrogenation during electrolysis.[14]

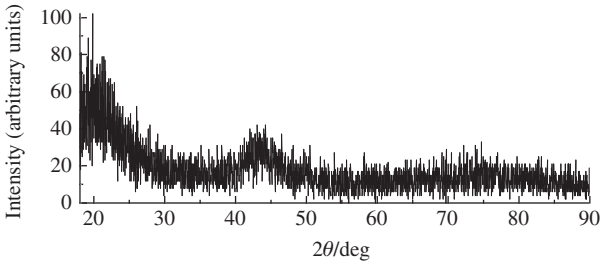

Figure 3 XRD pattern of the Fe–Mo alloy. E_{dep}, –1.00 V.

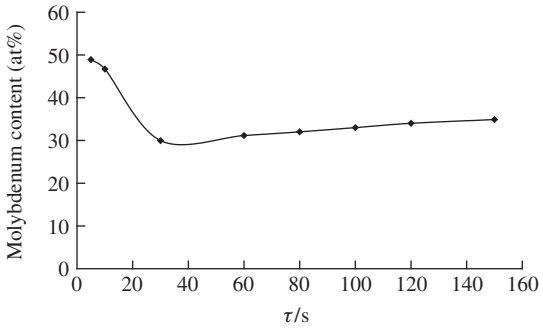

Figure 4 Dependence of the molybdenum content of Fe–Mo deposits on electrolysis time. E = –1.00 V, Cu substrate.

Potentiostatic transients (I–τ dependences) detected at all of the alloy electrodeposition potentials were characterized by a current minimum, which occurred 10–20 s after the beginning of electrolysis. The deposits obtained in the first seconds of electrolysis possessed a relatively high molybdenum content (Figure 4). It may be assumed that an adsorbed mixed-metal complex containing a significant amount of molybdenum was formed on the cathode surface at this time. This surface complex is essential for starting the electrochemical crystallization of alloy.[15] It was hypothesized[9] that molybdenum oxides are formed at the cathode at the initial stage of electrolysis. However, the results of this study indicated (Figure 4) that the deposits obtained in the first few seconds of electrolysis included not only molybdenum but also a considerable amounts of iron. Therefore, iron group metal ions enter into the composition of the surface intermediate formed at the cathode in the first seconds of electrolysis. Although molybdenum oxide compounds can also be included in the surface intermediate composition, the oxygen content of cathode deposits measured by XPS is no higher than 10 at%, which is much lower than the molybdenum content (~50 at%).

After ~40 s from the onset of electrolysis, the composition of cathode deposits was stabilized (Figure 4). The cathodic current (at E = const) also reached a constant value.

Hydrogen absorbed by Fe–Mo alloys during their electrodeposition was determined by a vacuum extraction technique (deposits were heat treated at 450 °C). Coatings were deposited to the surface of copper samples, assuming that copper absorbs negligible amounts of hydrogen.[16] Fe–Mo deposits were characterized by high concentrations of absorbed hydrogen (Table 3). The highest level of hydrogenation was observed in coatings obtained in the first minutes of electrolysis. However, even the deposits obtained over a period of 30 min were of high hydrogenation levels of 6–8 at%. This observation proves the hypothesis[14] that intense hydrogenation leads to the amorphization of molybdenum (tungsten)–iron group metal alloys (Figure 3). The hydrogen content of cathode deposits did not decrease when exposed to air. Even after Fe–Mo/Cu-samples had been stored for a year (at 20–25 °C), their hydrogen content was diminished only slightly (Table 3).

We are grateful to the Center of Materials Science and Metallurgy, the National University of Science and Technology MISIS for performing XPS analysis.

Table 3 Amounts of hydrogen sorbed by Fe–Mo deposits, i = 0.075 A cm^{-2}.

Time of electrolysis/ min	Hydrogen amount in the deposits (at%)	
	After electrodeposition	After a year of storage
5	16.1	—
10	10.7	—
20	6.2	4.8

References

1 E. G. Vinokurov and V. V. Bondar', *Protection of Metals and Physical Chemistry of Surfaces*, 2009, **45**, 369 (*Fizikokhim. Poverkhn. Zashchita Mater*., 2009, **45**, 334).
2 A. Boulaoued, I. Fechete, B. Donnio, M. Bernard, P. Turek and F. Garin, *Microporous Mesoporous Mater*., 2012, **155**, 131.
3 J.-L. Li, Y.-X. Zhang, C.-W. Liu and Q.-M. Zhu, *Catal. Today*, 1999, **51**, 195.
4 Z. Li, L.-T. Shen, W. Huang and K.-C. Xie, *J. Environ. Sci*., 2007, **19**, 1516.
5 F. Rosalbino, D. Maccio, A. Saccone, E. Angelini and S. Delfino, *Int. J. Hydrogen Energy*, 2011, **36**, 1965.
6 N. R. Elezovic, V. D. Jovic and N. V. Krstajic, *Electrochim. Acta*, 2005, **50**, 5594.
7 Z.-J. Niu, S.-B. Yao and S.-M. Zhou, *J. Electroanal. Chem*., 1998, **455**, 205.
8 V. V. Kuznetsov, K. E. Golyanin and T. V. Pshenichkina, *Russ. J. Electrochem*., 2012, **48**, 1107 (*Elektrokhimiya*, 2012, **48**, 1216).
9 E. Gómez, E. Pellicer and E. Vallés, *J. Electroanal. Chem*., 2005, **580**, 238.
10 E. G. Vinokurov and V. V. Bondar', *Theoretical Foundations of Chemical Engineering*, 2009, **43**, 293 (*Teor. Osnovy Khim. Tekhnol.*, 2009, **43**, 308).
11 V. S. Protsenko and F. I. Danilov, *Metal Finishing*, 2010, **108**, 28.
12 J. F. Moulder, W. F. Stickle, P. E. Sobol and K. D. Bomben, *Handbook of X-Ray Photoelectron Spectroscopy*, Perkin-Elmer Corporation, Eden Prairie, MN, 1992.
13 V. V. Kuznetsov, K. V. Kavyrshina and B. I. Podlovchenko, *Mendeleev Commun*., 2012, **22**, 206.
14 Yu. D. Gamburg and E. N. Zakharov, *Russ. J. Electrochem.*, 2008, **44**, 736 (*Elektrokhimiya*, 2008, **44**, 792).
15 E. J. Podlaha and D. Landolt, *J. Electrochem. Soc.*, 1997, **144**, 1672.
16 V. V. Gubin, L. T. Zhuravlev, B. M. Platonov and Yu. M. Polukarov, *Elektrokhimiya*, 1984, **20**, 715 (in Russian).

Received: 6th May 2013; Com. 13/4118